Quark Polarization at Small x

Matthew D. Sievert

with Yuri Kovchegov

and Daniel Pitonyak

7th Workshop of the APS Topical Group on Hadron Physics

Washington, D.C. Thu. Feb. 2, 2017

Overview: The Main Message

- Helicity PDF's obey novel, intricate small-x quantum evolution equations.

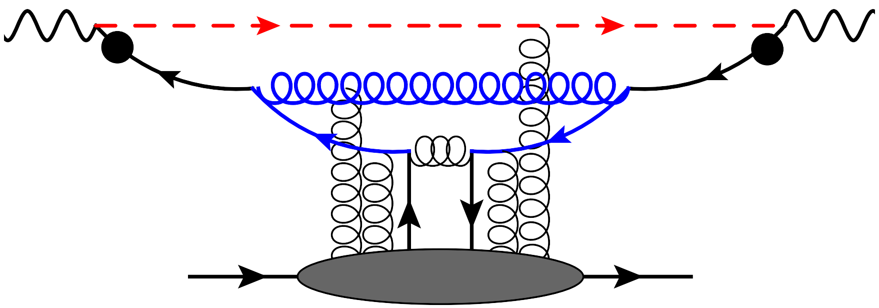

- Small-x evolution leads to a potentially sizeable contribution to the proton spin.

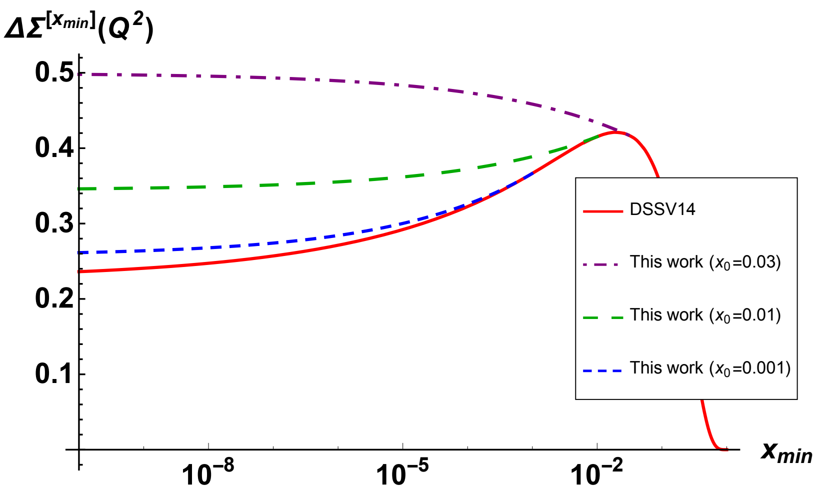

Yuri V. Kovchegov, Daniel Pitonyak, **M.S.**, Phys. Rev. **D95** (2017) 014033

Yuri V. Kovchegov, Daniel Pitonyak, **M.S.**, Phys. Rev. Lett. **118** (2017) 052001

Motivation: The Small-x Limit of PDF's

- Unpolarized PDF's show a power-law growth of gluons and sea quarks at small x due to (BFKL) quantum evolution.

- The cascade of small-x gluons drives up the color-charge density, enhancing multiple scattering.

- The high-density limit is characterized by the saturation of the gluon distribution.

Dulat et al., Phys. Rev. ***D93*** *(2016) no.3 033006*

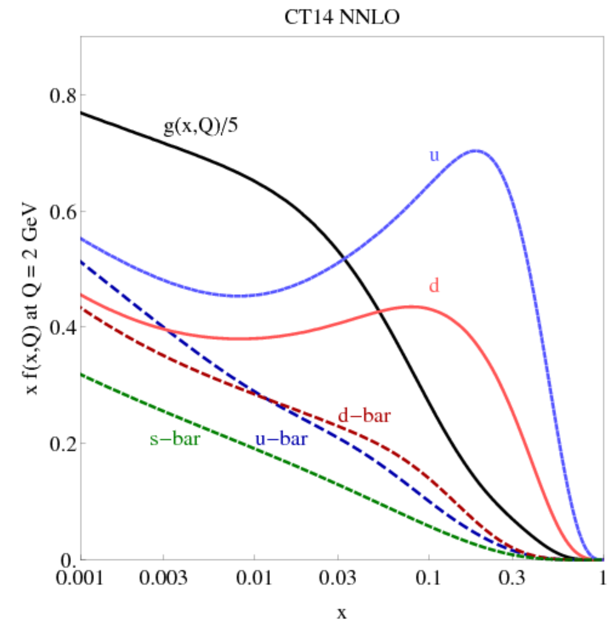

M.S., *Ph.D. Thesis, arXiv:1407.4047*

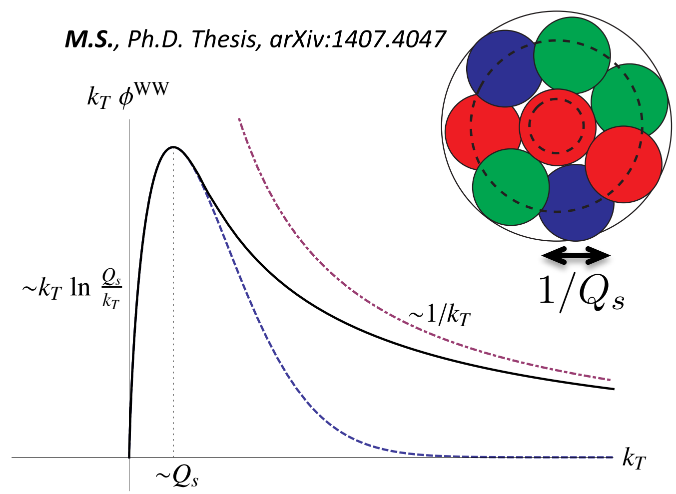

- In contrast, helicity PDF's are suppressed with power-law tails.
- The small-x evolution of helicity PDF's was studied by BER, predicting a growth at small x

Bartels, Ermolaev, and Ryskin, Z. Phys. ***C72*** *(1996) 627*

$$x\,\Delta q \sim \left(\frac{1}{x}\right)^{0.2} \quad \text{for} \quad Q^2 = 10\ GeV^2$$

- Could the small-x region make an important contribution to the proton spin?
- Could saturation physics be relevant?

de Florian et al., Phys. Rev. ***D80*** *(2009) 034030*

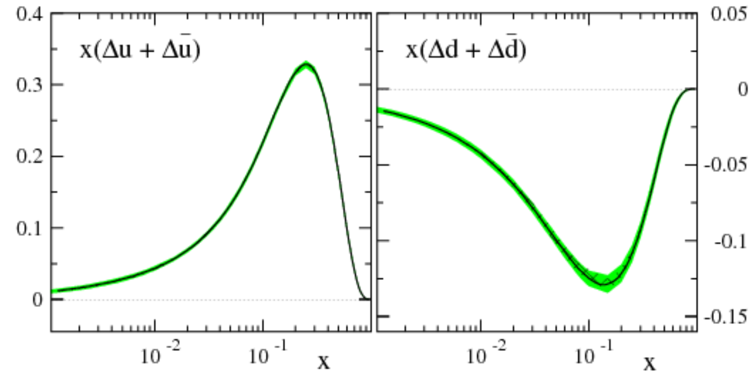

adapted from Aschenauer et al., Phys. Rev. ***D92*** *(2015) no.9 094030*

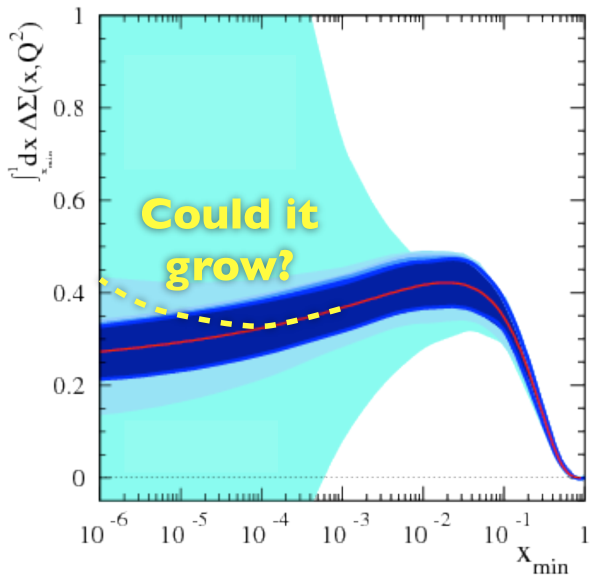

- In DIS at small x, quark dipole scattering dominates over quark "knockout".

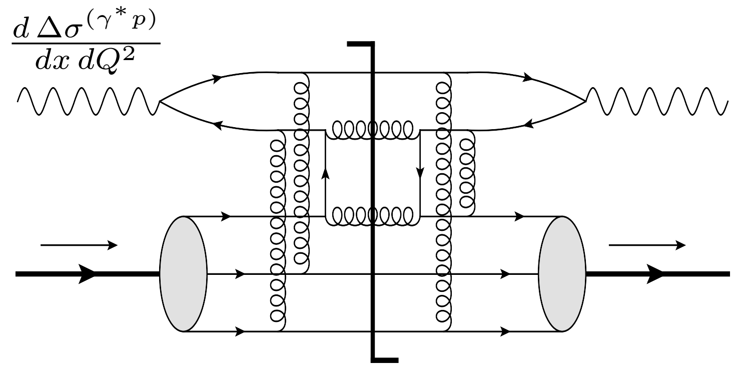

- PDF's at small x are described by dipole scattering amplitudes.

$$g_1(x, Q^2) = \int dr^- e^{ixp^+r^-} \langle pS|\bar{\psi}(0)\frac{\gamma^+\gamma^5}{2}\psi(r)|pS\rangle$$

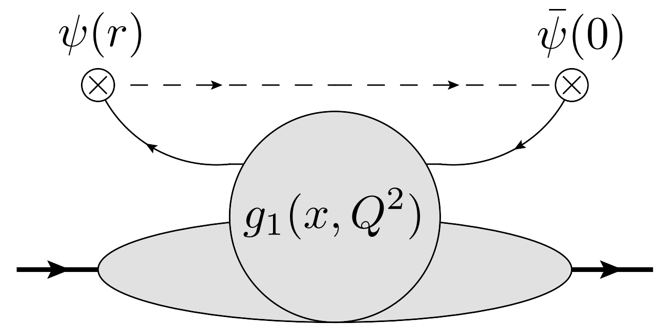

- Polarized PDF's at small x are described by polarized dipole scattering amplitudes.

$$V_{x_\perp}(\sigma) = V_{x_\perp} + \sigma V_{x_\perp}^{pol}$$

$$V_{x_\perp} = \mathcal{P}\exp\left[ig\int dx^+ \hat{A}^-(x^+, 0^-, x_\perp)\right]$$

$$V_{x_\perp}^{pol} \neq \mathcal{P}\exp\left[ig\int dx^+ \hat{A}^-(x^+, 0^-, x_\perp)\right]$$

The Polarized Dipole Amplitude

- Calculate the polarized dipole amplitude by relating it to a dipole cross-section.

- Explicitly scale out energy suppression of initial conditions:

$$G_{10} \equiv \frac{1}{2N_c} \langle\langle Tr[V_0 V_1^{pol\,\dagger} + V_1^{pol} V_0^{\dagger}] \rangle\rangle$$

$$= -\boxed{\frac{zs}{2}}\left[\boxed{\frac{d\sigma}{d^2b}}(q_0^{unp}, \Delta\bar{q}_1) + \boxed{\frac{d\sigma}{d^2b}}(\Delta q_1, \bar{q}_0^{unp})\right]$$

- Calculate the Born initial conditions to quantum evolution.

$$\vec{x}_{\perp,ij} \equiv \vec{x}_{\perp,i} - \vec{x}_{\perp,j}$$

$$\boxed{G^{(0)}(x_{10}^2, zs) = \frac{\alpha_s^2 C_F \pi}{N_c}\left[C_F \ln\frac{zs}{\Lambda^2} - 2\ln(zs\, x_{10}^2)\right]}$$

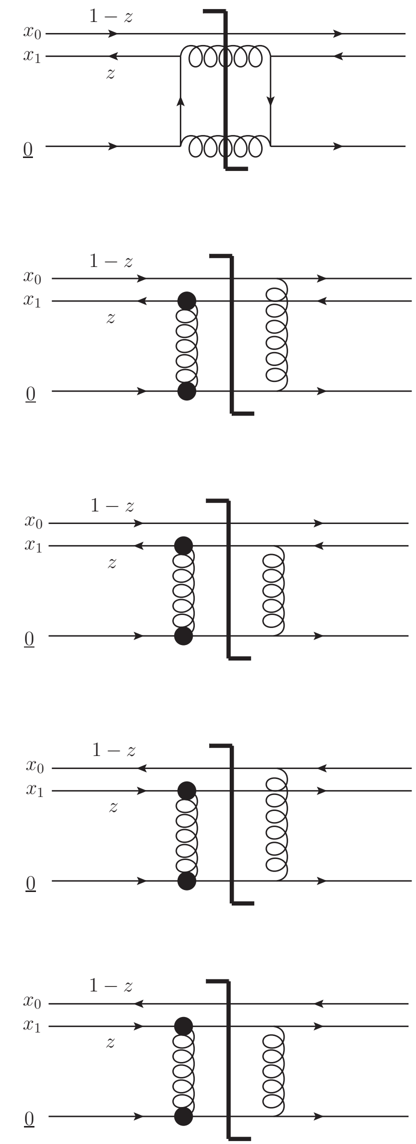

Origins of Helicity Evolution

- Helicity evolution is driven by parton splitting functions which transfer spin to small x.

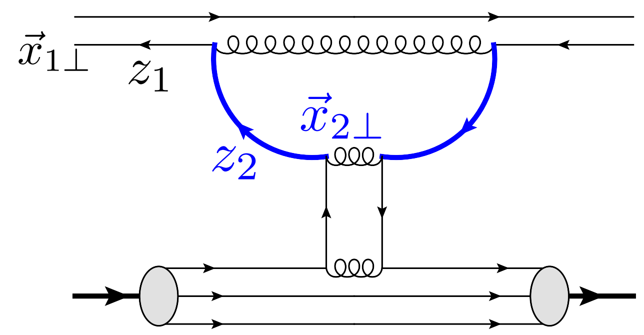

$$\underbrace{\left\langle V_1^{pol\,\dagger}(z_1)\right\rangle}_{\sim \frac{1}{z_1 s}} \sim \int \frac{dz_2}{z_2} \int d^2 x_2 \left(\frac{\alpha_s C_F}{2\pi^2} \frac{z_2}{z_1} \frac{1}{x_{21}^2} \right) \underbrace{\left\langle V_2^{pol\,\dagger}(z_2)\right\rangle}_{\sim \frac{1}{z_2 s}}$$

$$G_{10}(z_1) \sim \boxed{\frac{\alpha_s C_F}{2\pi} \int \frac{dz_2}{z_2} \int \frac{dx_{21}^2}{x_{21}^2}} G_{21}(z_2)$$

- Helicity evolution is double logarithmic, stronger than unpolarized evolution

$$\alpha_s \ln^2 \frac{1}{x} \sim 1$$

- Can strong quantum evolution reduce or offset the suppression of helicity at small x?

adapted from Aschenauer et al., Phys. Rev. ***D92*** *(2015) no.9 094030*

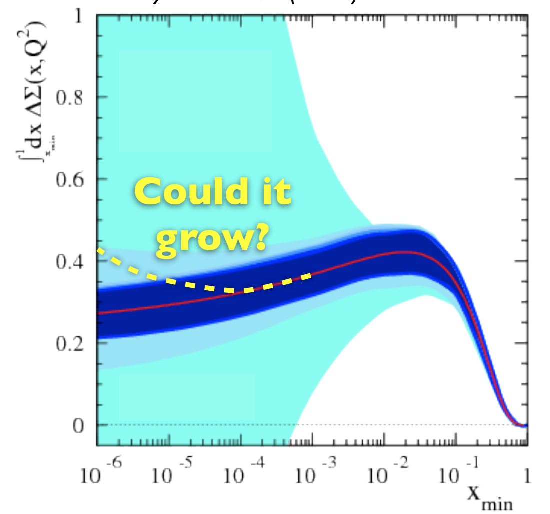

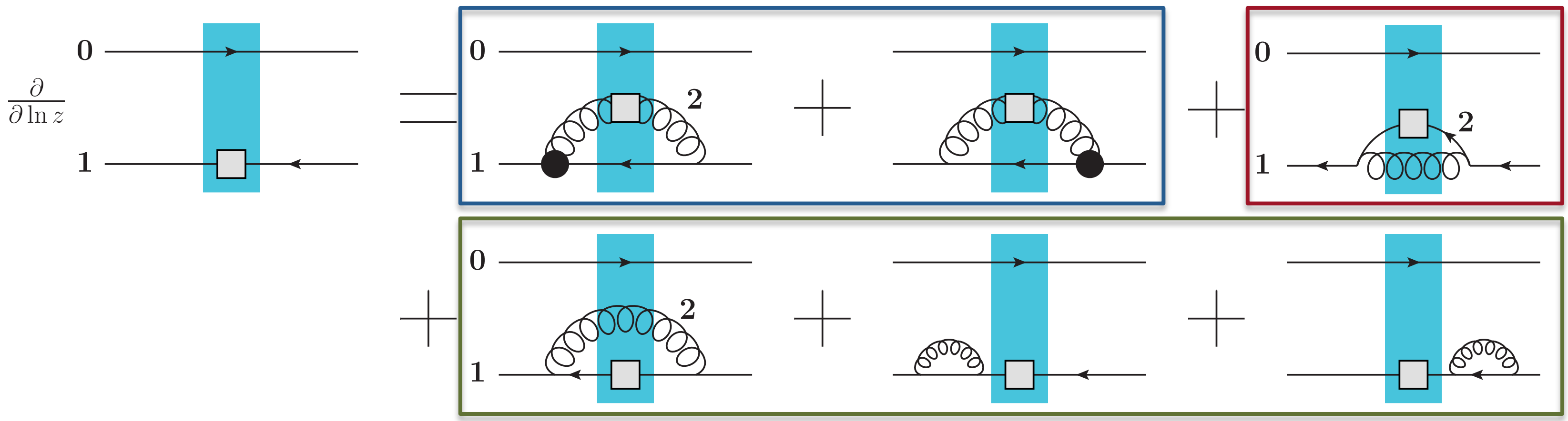

- Soft polarized gluon splitting: $\theta(x_{10}^2 - x_{21}^2)$
- Soft polarized quark splitting: $\theta(x_{10}^2 z - x_{21}^2 z')$ Infrared phase space!
- Soft unpolarized gluon splitting: $\theta(x_{10}^2 - x_{21}^2)$

The Need for Large-Nc Limit

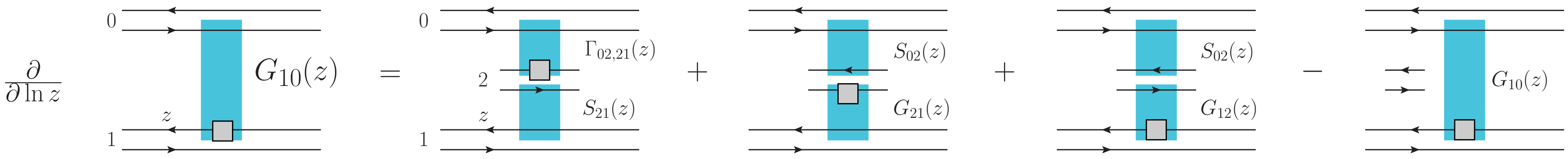

- Helicity evolution leads to an infinite hierarchy of operators

$$Tr[V_0 V_1^{pol\,\dagger}] \to \begin{cases} Tr[t^b V_0 t^a V_1^\dagger](U_2^{pol})^{ba} \\ Tr[V_0 V_1^\dagger]\, Tr[V_1 V_2^{pol\,\dagger}] \\ Tr[V_0 V_2^\dagger]\, Tr[V_2 V_1^{pol\,\dagger}] \end{cases}$$

- The large-Nc limit closes the hierarchy but neglects quarks

$$Tr[V_0 V_1^{pol\,\dagger}] \to Tr[V_0 V_1^{pol\,\dagger}]$$

- But due to competing phase spaces, not all dipoles are independent!

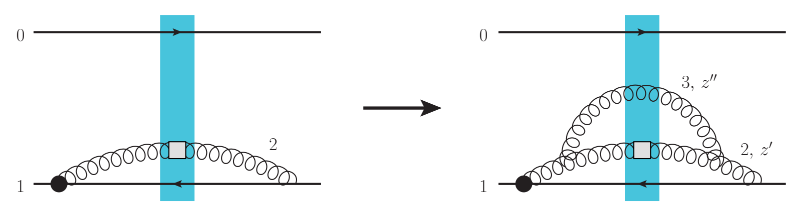

Dependence on a neighbor dipole's size!

$$x_{32}^2 z'' \ll x_{21}^2 z' \quad \text{vs.} \quad x_{32} \ll x_{02}^2$$

The Large-Nc Equations

$$G(x_{10}^2, z) = G^{(0)}(x_{10}^2, z) + \frac{\alpha_s N_c}{2\pi} \int\limits_{\frac{1}{x_{10}^2 s}}^{z} \frac{dz'}{z'} \int\limits_{\frac{1}{z' s}}^{x_{10}^2} \frac{dx_{21}^2}{x_{21}^2} \left[\Gamma(x_{10}^2, x_{21}^2, z') + 3 G(x_{21}^2, z') \right]$$

$$\Gamma(x_{10}^2, x_{21}^2, z') = G^{(0)}(x_{10}^2, z') + \frac{\alpha_s N_c}{2\pi} \int\limits_{\frac{1}{x_{10}^2 s}}^{z'} \frac{dz''}{z''} \int\limits_{\frac{1}{z'' s}}^{\min[x_{10}^2, x_{21}^2 \frac{z'}{z''}]} \frac{dx_{32}^2}{x_{32}^2} \left[\Gamma(x_{10}^2, x_{32}^2, z'') + 3 G(x_{32}^2, z'') \right]$$

- System of equations for the dipole + "neighbor dipole"
- Neighbor dipole differs due to competing phase space constraints
- Initial conditions: $G^{(0)}(x_{10}^2, zs) = \frac{\alpha_s^2 C_F \pi}{N_c} \left[C_F \ln \frac{zs}{\Lambda^2} - 2 \ln(zs\, x_{10}^2) \right]$

Attempting an Analytical Solution

$$G(s_{10},\eta) = G^{(0)}(s_{10},\eta) + \int_{s_{10}}^{\eta} d\eta' \int_{s_{10}}^{\eta'} ds_{21}[\Gamma(s_{10},s_{21},\eta') + 3G(s_{21},\eta')]$$

$$\Gamma(s_{10},s_{21},\eta') = G^{(0)}(s_{10},\eta') + \int_{s_{10}}^{\eta'} d\eta'' \int_{\max[s_{10},s_{21}+\eta''-\eta']}^{\eta''} ds_{32}[\Gamma(s_{10},s_{32},\eta'') + 3G(s_{32},\eta'')]$$

- Change to rescaled logarithmic variables
- Standard technique: Laplace/Mellin transform + saddle point approximation

$$s_{ij} \equiv \sqrt{\frac{\alpha_s N_c}{2\pi}} \ln \frac{1}{x_{ij}^2 \Lambda^2}$$

$$\eta^{(\prime,\prime\prime)} \equiv \sqrt{\frac{\alpha_s N_c}{2\pi}} \ln \frac{z^{(\prime,\prime\prime)}}{\Lambda^2/s}$$

$$G(s_{10},\eta) = \int \frac{d\omega}{2\pi i} e^{\omega\eta} \int \frac{d\lambda}{2\pi i} e^{\lambda s_{10}} G_{\omega\lambda} \longleftrightarrow G_{\omega\lambda} = \int_0^\infty ds_{10}\, e^{-\lambda s_{10}} \int_0^\infty d\eta\, e^{-\omega\eta}\, G(s_{10},\eta)$$

- Fails because the neighbor dipole couples the arguments in Mellin space!

Resorting to a Numerical Solution

- Resort to discretizing on a grid and solving numerically

$$\eta_i = i\,\Delta\eta \qquad i,j = 0 \cdots N \qquad N = \frac{\eta_{max}}{\Delta\eta}$$
$$s_j = j\,\Delta\eta$$

- Choose endpoints to allow an iterative solution

$$G_{ij} = G_{ij}^{(0)} + \Delta\eta^2 \sum_{j'=i}^{j-1} \sum_{i'=i}^{j'} [\Gamma_{ii'j'} + 3G_{i'j'}]$$

$$\Gamma_{ikj} = G_{ij}^{(0)} + \Delta\eta^2 \sum_{j'=i}^{j-1} \sum_{i'=max[i,k+j'-j]}^{j'} [\Gamma_{ii'j'} + 3G_{i'j'}]$$

- For fixed grid parameters $(\Delta\eta, \eta_{max})$, we can calculate the polarized dipole starting from the initial conditions at $\eta = 0$.

Extracting the Small-x Asymptotics

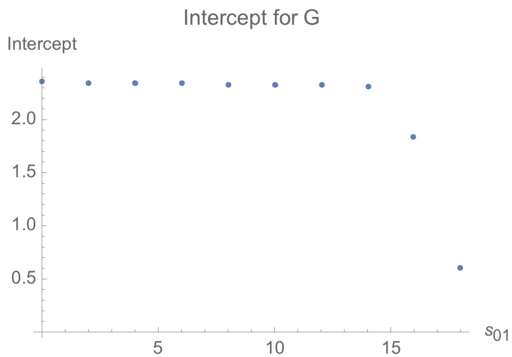

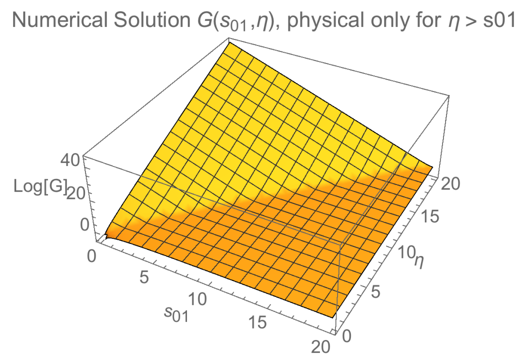

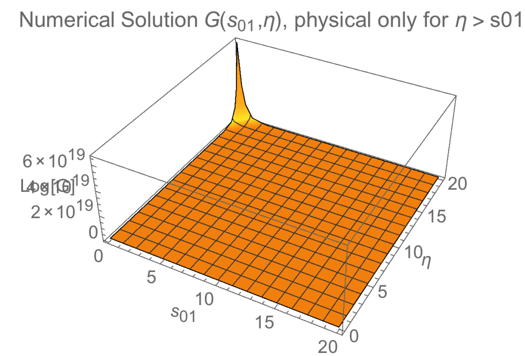

- Evolve in η until the asymptotic power-law behavior sets in.

$$G(zs) \sim \exp\left[\sqrt{\frac{2\pi}{\alpha_s N_c}}\alpha_h\,\eta\right] \sim (zs)^{\alpha_h}$$

- Fit the slope of $\ln G$ in the upper 25% of the η range to extract the intercept (power) α_h.

$$\alpha_h = \sqrt{\frac{\alpha_s N_c}{2\pi}}\frac{\partial}{\partial\eta}\ln G$$

- For a given set of grid parameters, we obtain the intercept

$$\boxed{\alpha_h(\Delta\eta, \eta_{max})}$$

Extrapolating to the Continuum

- We can scan the grid parameter space up to a computational limit on the grid size: $N = \frac{\eta_{max}}{\Delta\eta} = 500$

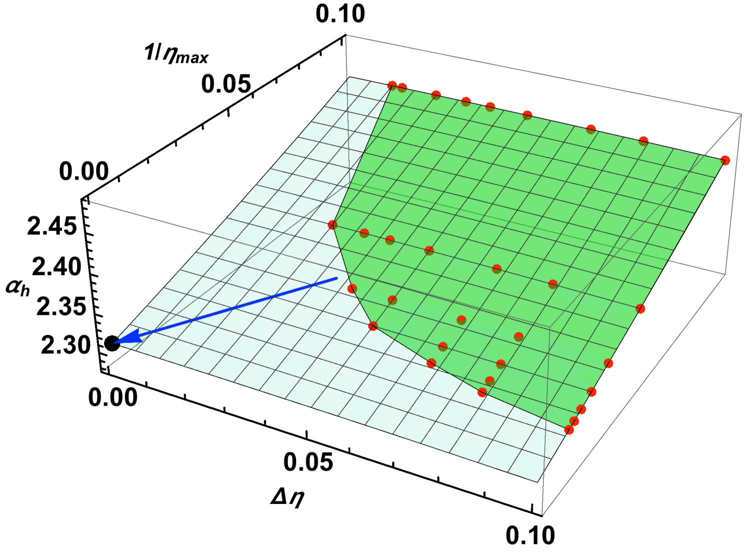

- The physical point is $(\Delta\eta, \eta_{max}) \to (0, \infty)$

- Fit all "data points" to a continuous function $\alpha_h(\Delta\eta, \eta_{max})$

$$\alpha_h(\Delta\eta, \eta_{max}) = A(\Delta\eta) + B(\Delta\eta)^2 + C(\tfrac{1}{\eta_{max}}) + D(\tfrac{1}{\eta_{max}})^2$$

$$\vdots$$

$$\alpha_h(\Delta\eta, \eta_{max}) = A(\Delta\eta)^B + C(\Delta\eta)^D + E(\Delta\eta \times \tfrac{1}{\eta_{max}})^F$$

- Use an AIC-weighted average to extrapolate to the physical point.

Akaike, IEEE Transactions on Automatic Control, ***19*** *(6) 716 (1974)*

Our Result: The Small-x Tail

$$\Delta q(x, Q^2) \sim \left(\frac{1}{x}\right)^{\alpha_h}$$

$$g_1(x, Q^2) \sim \left(\frac{1}{x}\right)^{\alpha_h}$$

$$\Delta\Sigma(Q^2) \equiv \int_0^1 dx\, \Delta q(x, Q^2) \sim \int_0 dx \left(\frac{1}{x}\right)^{\alpha_h}$$

Intercept

- Our results (flavor-singlet , pure glue, large-Nc):

$$\alpha_h = 2.31 \sqrt{\frac{\alpha_s N_c}{2\pi}}$$

- Fixed coupling:

$Q^2 = 3\ \text{GeV}^2$	$Q^2 = 10\ \text{GeV}^2$
$\alpha_h = 0.936$	$\alpha_h = 0.797$

- First QCD constraint on the small-x limit of the helicity PDF's!

- Flavor non-singlet case does not couple to gluons (40% smaller)

$$\alpha_h^{NS} = \sqrt{2} \sqrt{\frac{\alpha_s N_c}{2\pi}}$$

A Surprising Discrepancy

- Our results (pure glue, large-Nc):

$$\alpha_h = 2.31\sqrt{\frac{\alpha_s N_c}{2\pi}}$$

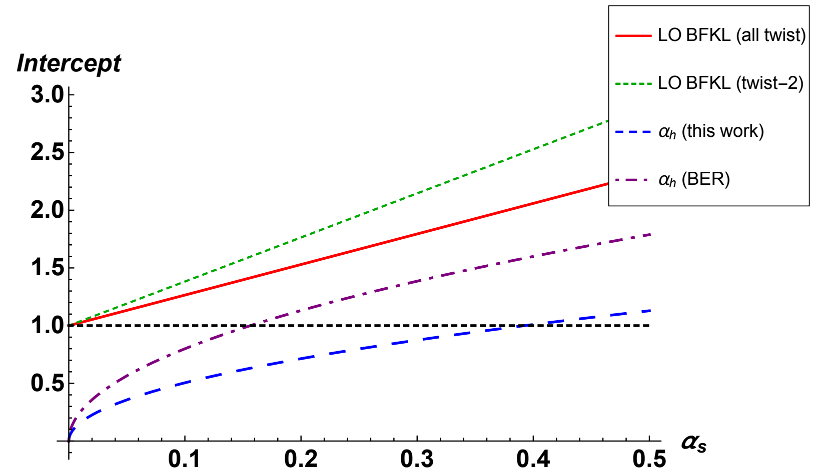

for $Q^2 = 10\ GeV^2$

Bartels, Ermolaev, and Ryskin, Z. Phys. ***C72*** *(1996) 627*

- BER (pure glue, Nc-independent):

$$\alpha_h = 3.66\sqrt{\frac{\alpha_s N_c}{2\pi}}$$

- Our intercept is 35% smaller than BER and generally integrable as $x \to 0$.

$$\Delta\Sigma = \int_0^1 dx\, \Delta q \sim \int_0 dx \left(\frac{1}{x}\right)^{0.80}$$

Us: converges!

$$\Delta\Sigma = \int_0^1 dx\, \Delta q \sim \int_0 dx \left(\frac{1}{x}\right)^{1.26}$$

BER: diverges!

- A similar decrease is seen from the all-twist to leading-twist BFKL intercept….

$$\alpha_P - 1 = \frac{\alpha_s N_c}{\pi} 4\ln 2 \qquad (\alpha_P - 1)_{L.T.} = \frac{\alpha_s N_c}{\pi}$$

Implications for the Proton Spin Puzzle

- Our intercept can be combined with PDF fits to estimate the small-x contribution to the proton spin.

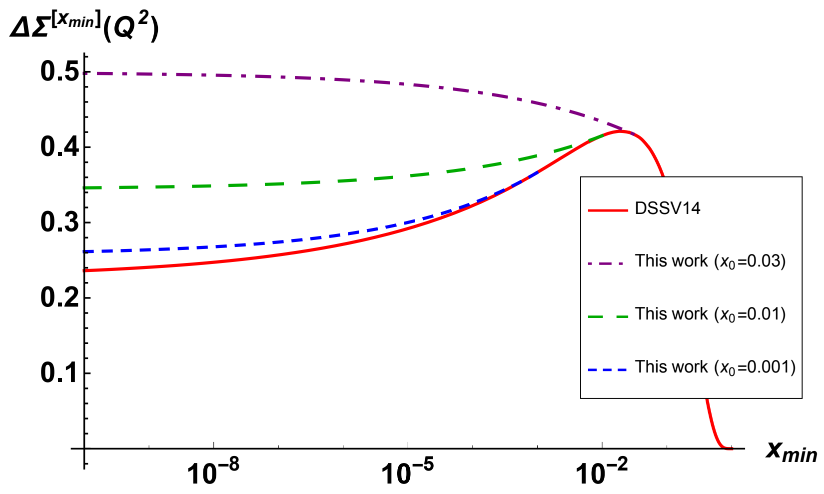

- The small-x tail can make a potentially large contribution!

- But… depends strongly on the approach to small x:
  - ➢ Onset of small-x behavior…
  - ➢ Assumptions about flavor symmetry in the sea…
  - ➢ Strange quark fragmentation functions…

Adolph et al., Phys. Lett. ***B753*** *(2016) 18*

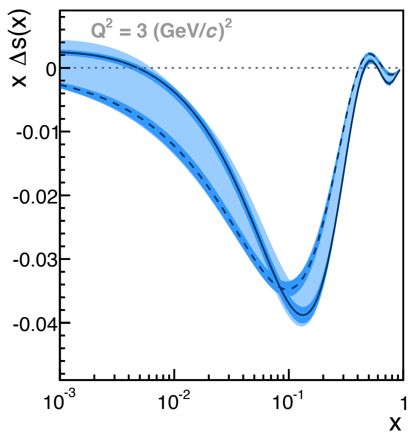

de Florian et al., Phys. Rev. ***D80*** *(2009) 034030*

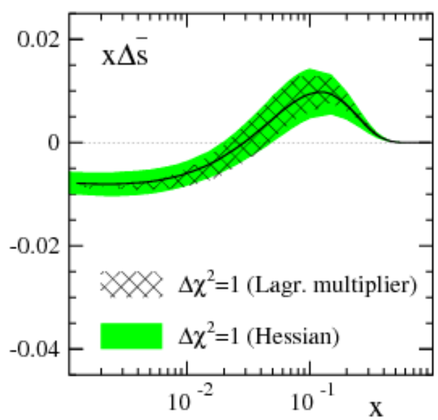

Conclusions

- Our numerical solution gives the first QCD constraints on the small-x asymptotics of helicity PDF's.
- The enhancement we find at small x is 35% smaller than in the literature.
- Can make a substantial contribution to the proton spin puzzle.
- This result needs to be incorporated from the ground level in the next-generation PDF fits.

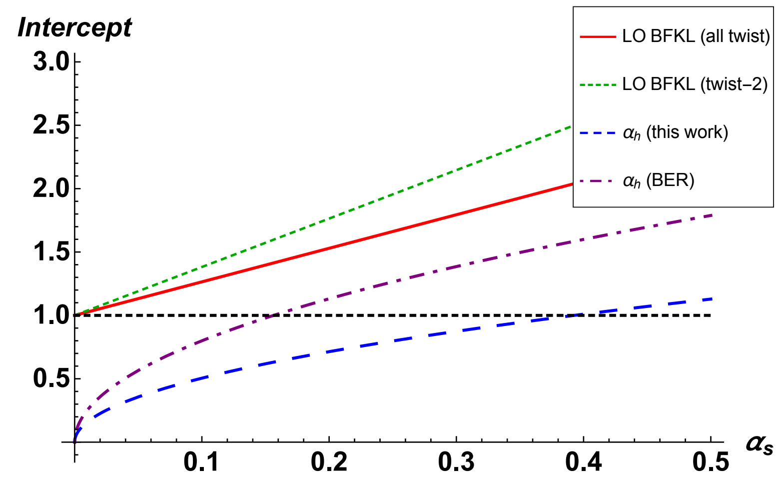

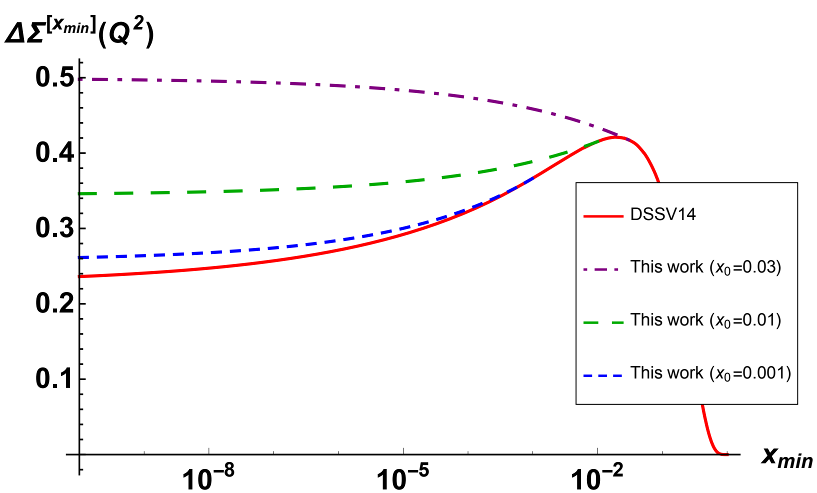

Outlook: Future Directions

- Does the gluon helicity PDF have the same small-x intercept? *(in progress)*

- Include quarks by taking the large Nc + Nf limit. *(cumbersome but straightforward)*

- Leading-log evolution and saturation corrections *(hard…)*

- Finite-Nc corrections *(hard…)*

- Other polarization observables *(the sky's the limit!)*

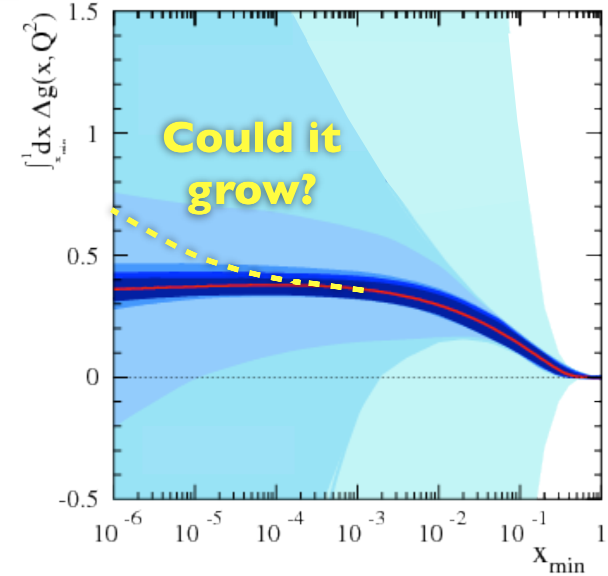

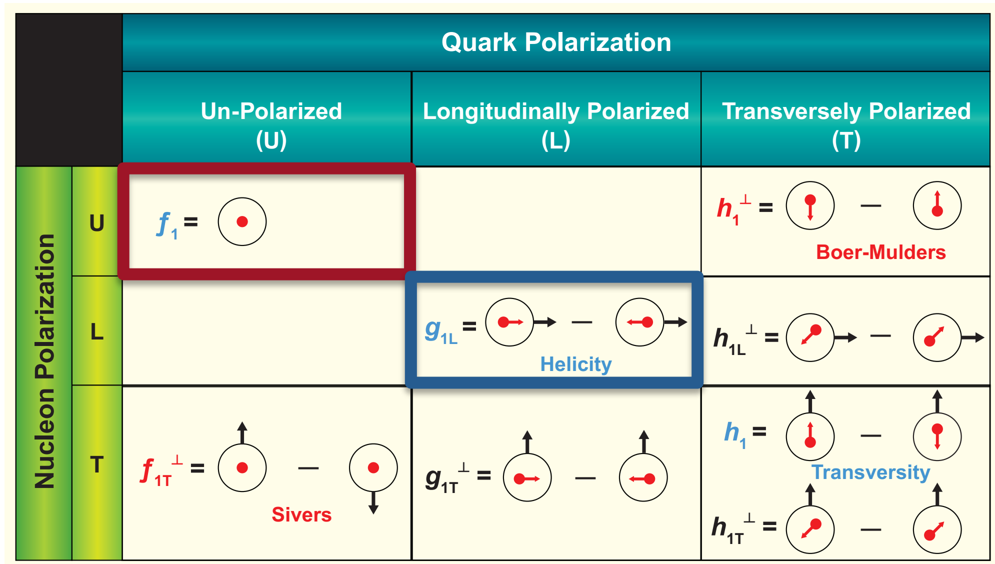

Backup Slides:

Applications: Transversity and BSM Physics

- One interesting sector is the quark transversity distribution.
  - ➢ Sum rule determines the proton tensor charge

*A. Courtoy et al., Phys. Rev. Lett. **115** (2015) 162001*

*T. Bhattacharya et al., Phys. Rev. Lett. **115** (2015) 212002*

- Tensor charge is sensitive to BSM physics through effective operators
  - ➢ Contribute to neutron EDM's
  - ➢ Mediate neutron beta decay

- Enhancement of transversity at small x?
  - ➢ Small-x evolution can help constrain the tensor charge.

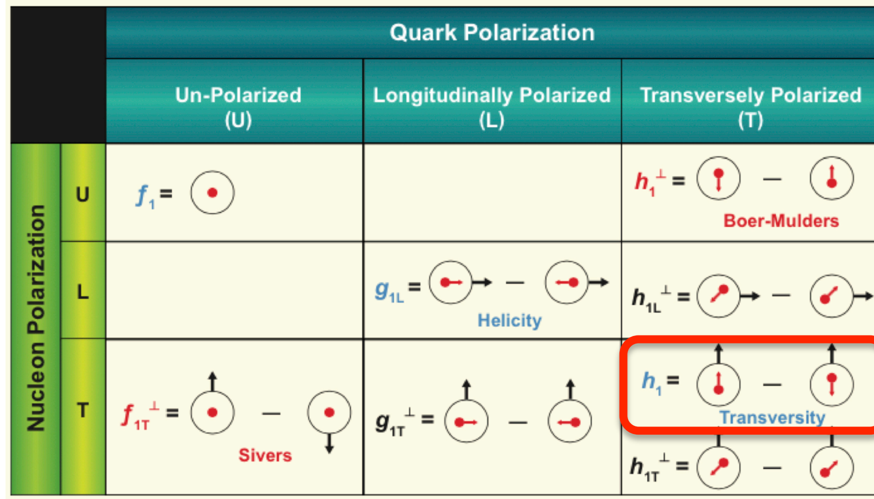

Tensor Charge:

$$g_T^q(Q^2) = \int_0^1 dx \, \left[h_1^q(x,Q^2) - h_1^{\bar{q}}(x,Q^2)\right]$$

Neutron EDM:

$$\langle n| \, \bar{\psi}(0) \, \sigma^{\mu\nu} \gamma^5 \, \psi(0) \, |n\rangle$$

Neutron Beta Decay:

$$\langle p| \, \bar{u}(0) \, \sigma^{\mu\nu} \gamma^5 \, d(0) \, |n\rangle$$

Applications: Higher-Order Corrections

- Polarized evolution currently only accurate to the leading (double) log
  - Can be systematically extended to higher orders

Flavor-changing Wilson lines at finite N_c:

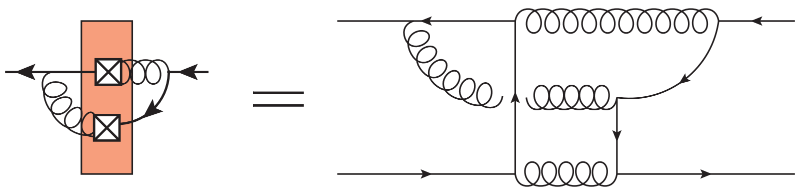

- Important physical corrections:
  - Quark exchange (large N_c + N_f)
  - NLL (single-log corrections and saturation)
  - Running coupling (reduces enhancement)

Fixed vs. Running BK Evolution:

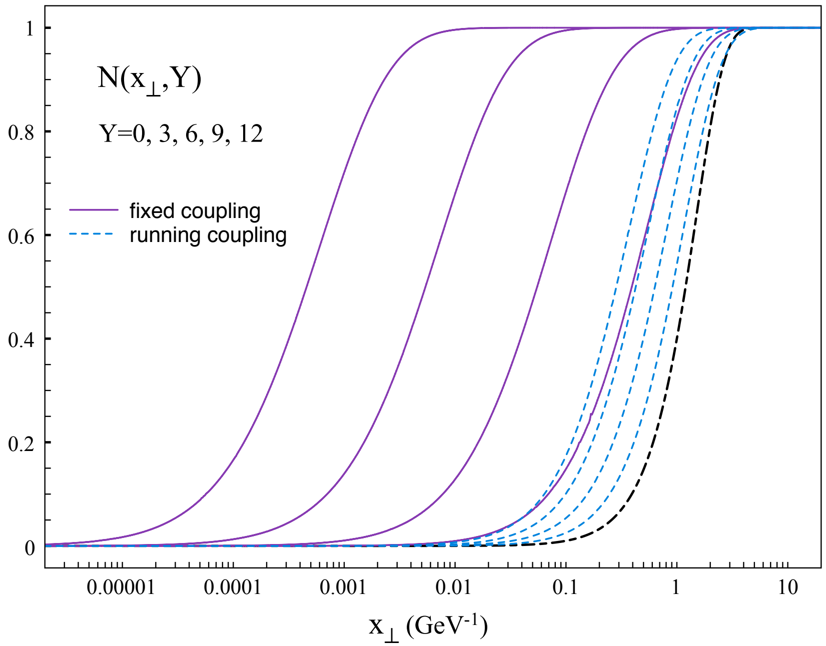

- Any / all of these may be important before confidently matching to data.

What Do BER Do?

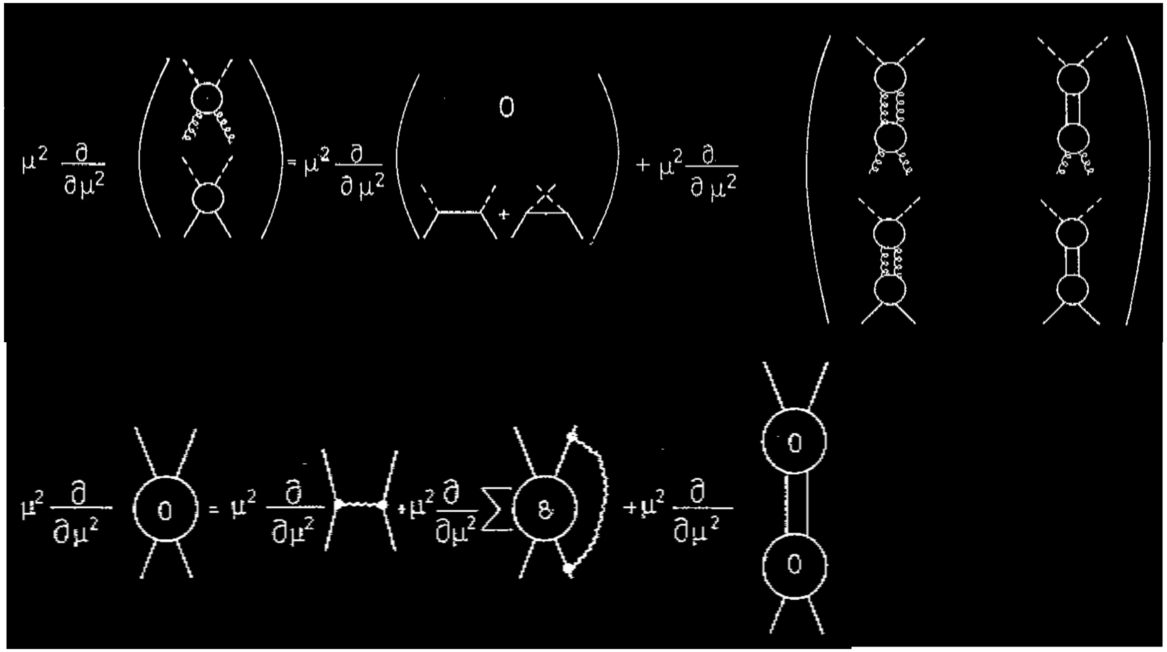

Bartels et al.,
Z. Phys. ***C72*** *(1996) 627*

- Attempt to re-sum mixed logarithms of x and Q^2.

$$(\alpha_s)^n [b_n (\ln(1/x))^{2n} + b_{n-1} (\ln(1/x))^{2n-1} \ln(Q^2/\mu^2) + \ldots + b_0 (\ln(1/x))^n (\ln(Q^2/\mu^2))^n$$

- They also have both ladder and non-ladder gluons (the primary source of our complexity)

- Their calculation uses Feynman gauge (we use light-cone gauge).

What are BER's Equations?

- Transform the spin-dependent part of the hadronic tensor to Mellin space:

$$T_3 = \int_{-i\infty}^{i\infty} \frac{d\omega}{2\pi i} (\frac{s}{\mu^2})^\omega \xi_(\omega) R(\omega, y)$$

- Write down "infrared evolution equations" in Mellin space:

$$(\omega + \frac{\partial}{\partial y}) R = \frac{1}{8\pi^2} F_0 R \qquad y = \ln(\frac{Q^2}{\mu^2})$$

- Obtained coupled matrix equations which can be solved analytically

$$F_0 = \begin{pmatrix} F_{gg} & F_{qg} \\ F_{gq} & F_{qq} \end{pmatrix} \quad M_0 = \begin{pmatrix} 4C_A & -2T_f \\ 2C_F & C_F \end{pmatrix}$$

$$G_0 = \begin{pmatrix} C_A & 0 \\ 0 & C_F \end{pmatrix} \quad M_8 = \begin{pmatrix} 2C_A & -T_f \\ C_A & -1/2N \end{pmatrix}$$

$$F_0(\omega) = \frac{g^2}{\omega} M_0 - \frac{g^2}{2\pi^2\omega^2} G_0 F_8(\omega) + \frac{1}{8\pi^2\omega} F_0(\omega)^2$$

$$F_8 = \frac{g^2}{\omega} M_8 + \frac{g^2 C_A}{8\pi^2\omega} \frac{d}{d\omega} F_8(\omega) + \frac{1}{8\pi^2\omega} F_8(\omega)^2$$

BER's Solution

- They obtain an analytic expression, with the intercept determined by the eigenvalues of their matrices.

$$g_1(x, Q^2) = \frac{\omega_s^{3/2}}{8\sqrt{2\pi}} \frac{\frac{2}{\omega_s} + \ln Q^2/\mu^2}{(\ln(1/x))^{3/2}} (\Delta g, \Delta\Sigma) R(\omega_s, y) \boxed{(\frac{1}{x})^{\omega_s}} \left(1 + O(\frac{\ln^2 Q^2/\mu^2}{\ln 1/x})\right)$$

$$\omega_s = z_s \sqrt{\alpha_s N_c / 2\pi}$$

$z_s = 3.45 \qquad (n_f = 4)$

$z = 3.66$ pure glue

- But all the complexity actually only leads to a small effect compared to the ladder graphs.

Ladder only:

$z_s = 3.81 \qquad (n_f = 4)$

$z_s = 4$ pure glue

- We agree on the ladder part, but we seem to include additional diagrams which lead to a larger effect.

Diagrammatic Discrepancies

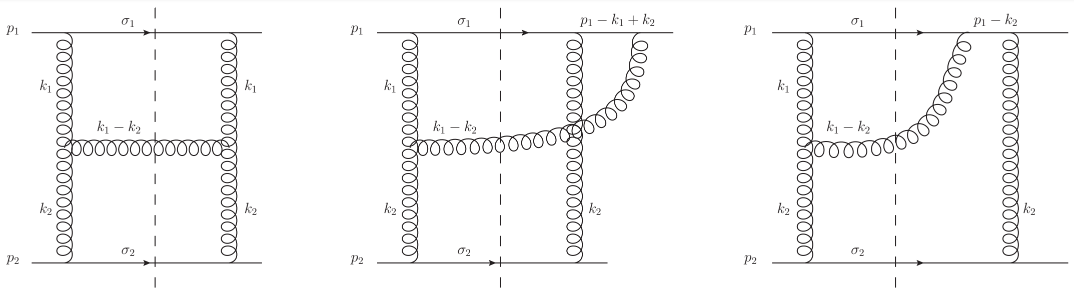

A B C

Us: All Cancel

BER: B+C = 0 for $k_{2T}^2 \gg k_{1T}^2$,
A = nonvanishing contribution

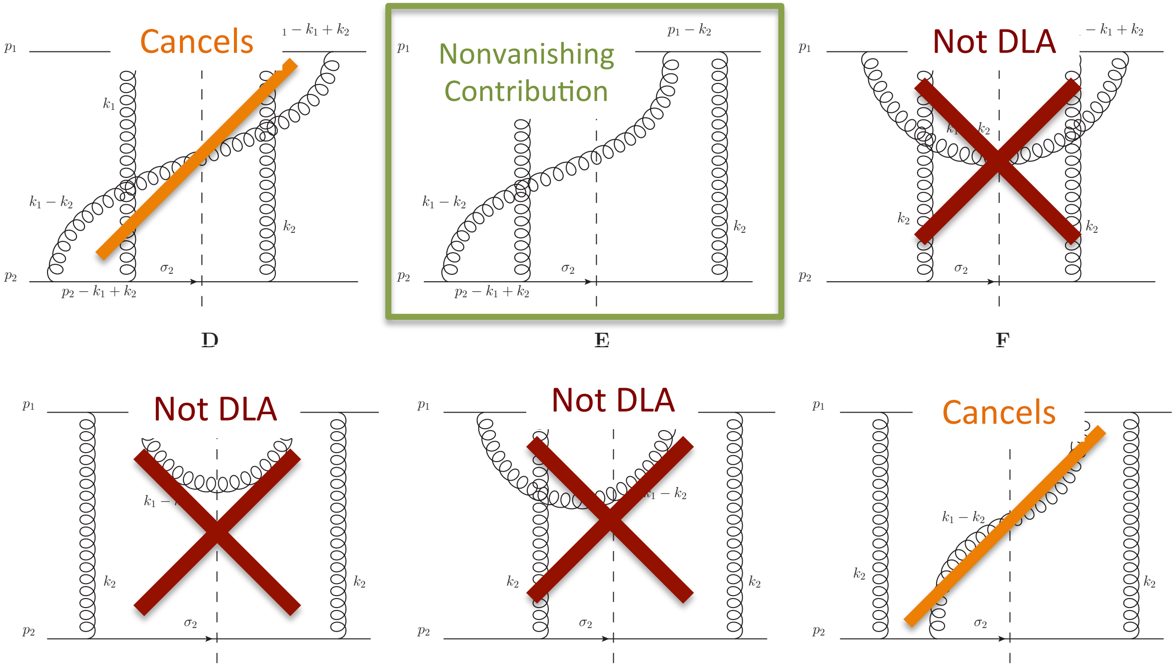

D E F

G H I

Not considered by BER?

Anomalous Dimensions

- They reproduce the DGLAP anomalous dimensions to NLO (and beyond)…

$$\gamma_S^{(1)} = \left(\frac{\alpha_s}{4\pi}\right)^2 \frac{1}{\omega^3} \begin{pmatrix} \boxed{32C_A^2} - 16C_F T_f & -16C_A T_f - 8C_F T_f \\ 16C_A C_F + 8C_F^2 & 4C_F^2 - 16C_F T_f + \frac{8C_F}{N} \end{pmatrix}$$

- We also reproduce the G/G anomalous dimension in the large-Nc limit…

$$\gamma_{S,GG}^{(1)}(\omega) = \left(\frac{\alpha_s}{2\pi}\right)^2 8N_c^2 \frac{1}{\omega^3}$$

- Whatever diagrams they exclude do not miss any leading logarithms of Q^2…

- Perhaps our disagreement is over higher-twist corrections? That would explain our 35% smaller intercept….
  - Unpolarized sector: $\frac{1}{4\ln 2} \approx 36\%$